



# Groundwater level prediction based on GMS and SVR models under climate change conditions: Case Study—Talesh Plain

Reza Seraj Ebrahimi<sup>1</sup> · Saeid Eslamian<sup>1,2</sup> · Mohammad Javad Zareian<sup>3</sup>

Received: 12 February 2022 / Accepted: 11 November 2022

© The Author(s), under exclusive licence to Springer-Verlag GmbH Austria, part of Springer Nature 2022

## Abstract

This study compared the capability of GMS and SVR models for groundwater modeling and evaluated the impact of climate change on future aquifer quantity in Talesh Plain. Groundwater level modeling was performed using GMS and SVR models for the period 2005–2018 (base period). Also, the effects of climate change on temperature and precipitation in the study area were estimated based on the HadGEM2-ES GCM model considering RCP 2.6, RCP 4.5, and RCP 8.5 emission scenarios in 2020–2034 (future period). A correlation of greater than 0.70 was found between the observed and estimated groundwater levels in both models. Moreover, in the base period, the average decline in groundwater level was 0.86 m. SVR model exhibited that the average groundwater level will drop by 0.94, 0.98, and 1.04 m in RCP2.6, RCP4.5, and RCP8.5 emission scenarios, respectively. While in the GMS modeling, under the same emission scenarios, these values were 0.91, 0.95, and 1.06 m, respectively. Moreover, the current trend of groundwater withdrawal may significantly increase the groundwater deficit and aquifer imbalance. It is therefore essential to apply artificial intelligence and mathematical models to accurately predict groundwater level fluctuations in this region to optimize groundwater management. Overall, our results revealed that SVR and GMS models perform almost similarly in simulating groundwater levels in the study area, suggesting that artificial intelligence can serve as a fast decision-making tool in groundwater management in similar aquifers.

## 1 Introduction

Groundwater, as an easily accessible and inexpensive water resource that constitutes an important part of the world's freshwater resources, is extensively extracted from groundwater aquifers in various regions of the world. This excessive withdrawal has led to a drop in groundwater levels in various aquifers, especially in arid regions. These groundwater crises have been exacerbated by climate change and

population growth (which has increased water demand) (Koutsoyiannis 2020). Water quantity vulnerability can be defined as the sensitivity of the aquifer to a certain level of groundwater withdrawal at a specific time (Barzegar et al. 2021; Zaghayan et al. 2021). Thus, the groundwater level is a critical parameter that must be considered to achieve sustainable groundwater management. However, this vital parameter may fluctuate due to changes in several components such as climate variability, water withdrawal, aquifer recharge, and so on (Usman et al. 2020; Minnig et al. 2018; Wakode et al. 2018).

Based on the predictions of the Global Climate Models (GCMs), the global annual average temperature by 2100 will be between 1.5 and 7.8 °C warmer than in the period 1850–1900 as a result of various greenhouse gas emission scenarios (Pachauri et al. 2014). Another negative impact of climate change is the change in global precipitation patterns, leading to an increase in the intensity, duration, and frequency of severe weather events in the future, and may lead to significant changes in extreme events such as floods and long-term droughts (Filipe et al. 2013). Since hydrological and environmental phenomena occur with a time lag compared to meteorological phenomena; consequently,

✉ Saeid Eslamian  
saeid@cc.iut.ac.ir

Reza Seraj Ebrahimi  
reza\_serajebrahimi@yahoo.com

Mohammad Javad Zareian  
m.zareian@wri.ac.ir

<sup>1</sup> Department of Civil Engineering, Najafabad Branch, Islamic Azad University, Najafabad, Iran

<sup>2</sup> Department of Water Engineering, College of Agriculture, Isfahan University of Technology, Isfahan, Iran

<sup>3</sup> Department of Water Resources Study and Research, Water Research Institute (WRI), Tehran, Iran

climate change may cause unforeseen effects on other phenomena affecting the water cycle and environmental factors such as precipitation infiltration, surface runoff, evaporation and land cover, and so on. These phenomena may also influence the quantity and quality of groundwater resources (Sharafati et al. 2020; Cuthbert et al. 2019; Trichakis et al. 2011; Döll 2009). Moreover, the effects of global warming and climate change on the hydrosphere and biosphere are currently being observed, threatening the sustainability of water resources and ecosystems (Liu et al. 2020). Therefore, sustainable water supply for the domestic, industrial, environmental, and agricultural water demands in the face of climate change is one of the most important challenges of the twenty-first century. Policymakers are strongly focused on using modern scientific tools and techniques, one of the basic strategies, for managing and planning sustainable water resources to meet this challenge (Gohari et al. 2017; Eslamian et al. 2017).

To develop sustainable management strategies for water resources, groundwater modeling has become increasingly popular in recent decades as an efficient, dynamic, and scientific tool. Water resources research and management are increasingly faced with the challenge of modeling groundwater cycles because aquifers exhibit considerable spatial and temporal variability. Furthermore, there is a highly complicated and nonlinear relationship between climate variables (i.e., precipitation, temperature, pumping, evaporation, and transpiration) and groundwater levels. Therefore, monitoring and managing groundwater levels in different aquifers using available limited and local data are subject to large uncertainties. Despite the widespread use of spatial interpolation techniques (such as kriging and inverse distance weighting (IDW)) to zone meteorological and hydrological variables, these statistical gaps cannot be filled because these techniques are most effective in areas with uniformly distributed and dense local data (Cui et al. 2021; Dehghan et al. 2019 and Dehghan et al. 2020). In other words, it is more challenging in areas where there are limited observations and most data are confined to a few specific areas of the study area.

There are two general frameworks for groundwater studies and simulations. First, artificial intelligence and GIS techniques have been used in several studies to predict groundwater level variations in different hydrogeologic environments. Second, physics-based models (e.g., MODFLOW, MT3DMS, SEAWAT, FEMWATER) are the other tools that are used as alternative methods for quantitative and qualitative groundwater modeling under different scenarios such as human activities and climate change. Over the past few decades, groundwater dynamics have been modeled using the latter models (Lal and Datta 2019; Mahmoodzadeh and Karamouz 2019; Voss and Souza 1987; Yu and Michael 2019). These models are designed based on a detailed

description of the groundwater process (e.g., Richards and convection–dispersion equations) and can provide a mechanical understanding of groundwater physical processes at both small and regional scales (Pham and Tsai 2016). Groundwater balance is typically determined using experimental equations or mathematical modeling such as MODFLOW (Javadi et al. 2021). Although process-based (or physical) models provide an efficient tool for modeling complex natural systems (such as groundwater systems), access to extensive and accurate data is crucial for the development of process-based groundwater flow/transfer models. This lack of data and information is a major limitation in most studies. Other methods are data-driven techniques, which are based on the relationships between the inputs and outputs of observational data without requiring parameters or data about the underlying processes in the system (ASCE 2000). Accordingly, these models are classified as “experimental models” frameworks.

Recently, artificial intelligence methods, such as artificial neural network (ANN), adaptive neuro-fuzzy inference system (ANFIS), genetic programming (GP), support vector machine (SVM), extreme learning machine (ELM), and (SVR), have been widely used to predict Hydrology/Hydrogeology-dependent variables due to their ability to recognize complex mathematical relationships between target and predictor variables (Daliakopoulos et al. 2005; Mao et al. 2002; Nourani et al. 2008; Rakhshandehroo et al. 2012; Sreekanth et al. 2009; Trichakis et al. 2011; Affandi and Watanabe 2007; Emamgholizadeh et al. 2014; Fallah-Mehdipour et al. 2014, 2013; Jalalkamali et al. 2011; Kasiviswanathan et al. 2016; Maiti and Tiwari 2014; Mayilvaganan and Naidu 2011; Yoon et al. 2011, 2011; AliNejad et al. 2021; Savichev et al. 2021; Yadav et al. 2017). The application of these methods does not require detailed information on the physical properties of the aquifers. In other words, they can simulate the relationships between groundwater-introducing variables (such as groundwater level) and the variables affecting them based on mathematical and logical relationships. Hence, recently machine learning methods are increasingly being used to estimate groundwater levels (Chen et al. 2020; Rahman et al. 2020; Sahoo et al. 2017), regionalize the potential groundwater recharge (Pourghasemi et al. 2020), assess groundwater vulnerability (Moazamnia et al. 2020; Moghaddam et al. 2020), and forecast groundwater quality (Li et al. 2020; Liu et al. 2017; Rahmati et al. 2019). The use of machine learning methods has therefore become widely adopted in groundwater research. Compared with the physical simulation of aquifers, these methods require fewer input data and less computational time while providing acceptable results (Sajedi-Hosseini et al. 2018; Ren et al. 2018). Furthermore, various studies have investigated the groundwater level fluctuations

under the influence of different factors using analytical solutions, finite element, and finite difference codes (Alcaraz et al. 2016; Molina-Giraldo et al. 2011; Choi et al. 2011; Langevin et al. 2010; Somogyi et al. 2015) and divergent hydrological and hydrogeological models such as MT3DMS, MODFLOW, FEFLOW, and HYDRUS (Harbaugh et al. 2000; Zheng and Wang 1999; Diersch 2005; Simunek et al. 2016). Accordingly, accurate methods should be used at regional- and large scales to study the trend of groundwater level fluctuations to assist water resource decision makers in their decisions.

In many regions of the world, groundwater has declined as a result of excessive withdrawals and inadequate conservation measures. Additionally, droughts have put more pressure on water resources in arid regions of the world, making optimal use of water resources a major concern. Consequently, there is a serious need for sustainable groundwater management in these regions (Chezgi et al. 2016; Das and Pal 2020; Lu et al. 2019; Feng et al. 2020; Nguyen et al. 2020). Managing strategies to conserve these valuable water resources in the future will therefore require careful spatial monitoring of groundwater aquifers (Chen et al. 2018; Nosrati and Van Den Eeckhaut 2012). A coastal aquifer (Talesh Plain) is selected for this study, and since many of the rivers in such areas are not of high quality due to seawater infiltration, groundwater resources could serve as a suitable alternative for providing freshwater for domestic, industrial, and agricultural use (Kaur et al. 2020; Mohanty and Rao 2019). Although this region receives significant amounts of precipitation, due to the lack of high-quality surface water, groundwater resources are also used extensively in many areas (especially for agriculture). Consequently, the groundwater level in this area has decreased in recent years, posing major risks including saltwater intrusion into aquifers and declining groundwater quality. The coincidence of these conditions with climate change has raised many concerns about the future socioeconomic conditions of this important agricultural hub, which is one of the most important rice-growing areas in Iran (Mahmoudpour et al. 2021; Al-Sheikh et al. 2004). It can therefore be vital to develop regional water management programs in this sensitive region by studying the effects of climate change on groundwater resources. Thereby, artificial intelligence-based models such as Support Vector Regression (SVR) and GMS were used to study and manage groundwater levels under the influence of different scenarios (including climatic scenarios and water withdrawal scenarios). Accordingly, this study aimed two key objectives, including (a) comparison of the Groundwater Modelling System (GMS) and Support Vector Regression (SVR) models' ability to investigate groundwater level fluctuations in Talesh Plain and (b) estimating the impact of climate change on aquifer level fluctuations in future periods (2020–2034).

## 2 Materials and methods

### 2.1 Study area

The Talesh Plain is located in the northwest of Gilan Province in northern Iran and has an area of 488.02 km<sup>2</sup> (48° 48' 5" to 49° 11' 15" E, 37° 31' 35" to 38° 27' 2" N, between 26 and 76 m above sea level) (Fig. 1). This region has a humid and semi-humid climate, with an average annual precipitation of 1139.7 mm/year (Mahmoudpour et al. 2021; Al-Sheikh et al. 2004). This area has good annual precipitation, but surface water resources are inadequate for the various water-using sectors in the area, resulting in significant groundwater withdrawal. Moreover, the proximity of the Talesh aquifer to the sea poses a threat to seawater infiltration because the aquifer is over-drained. Therefore, groundwater management in this region is also very important, and its neglect may lead to the degradation of the quantity and quality of groundwater resources in the area.

### 2.2 Data preparation

For this study, various meteorological, hydrological, and hydrogeological data were collected from different organizations. Accordingly, river flow and flow in irrigation channels (key factors to estimate groundwater recharge and create boundary conditions for the model), geometric data (such as a river, aquifers, and irrigation canals boundaries), pumping wells, and various aquifer characteristics during the period (2005–2018) were prepared by the Water Resources Management Organization of Iran (Table 1 and Fig. 2). Furthermore, meteorological data (including maximum and minimum air temperature, precipitation, evapotranspiration) during the period (1992–2020) were provided by the Meteorological Organization of Iran.

### 2.3 Climate change

In this study, daily precipitation and temperature data were collected from Talesh synoptic station to investigate climate change. Due to the multiplicity of General Circulation Models (GCMs), the HadGEM2-ES model (from the fifth IPCC assessment model (CMIP5)) was used to assess the climate change impacts in the study area. Three emission scenarios RCP2.6, RCP4.5, and RCP8.5 were used to predict the effects of the climatic phenomenon on temperature and precipitation in the study area (RCP: Representative Concentration Pathway). These emission scenarios differ in their radiative forcing, with RCP8.5 having the highest level and

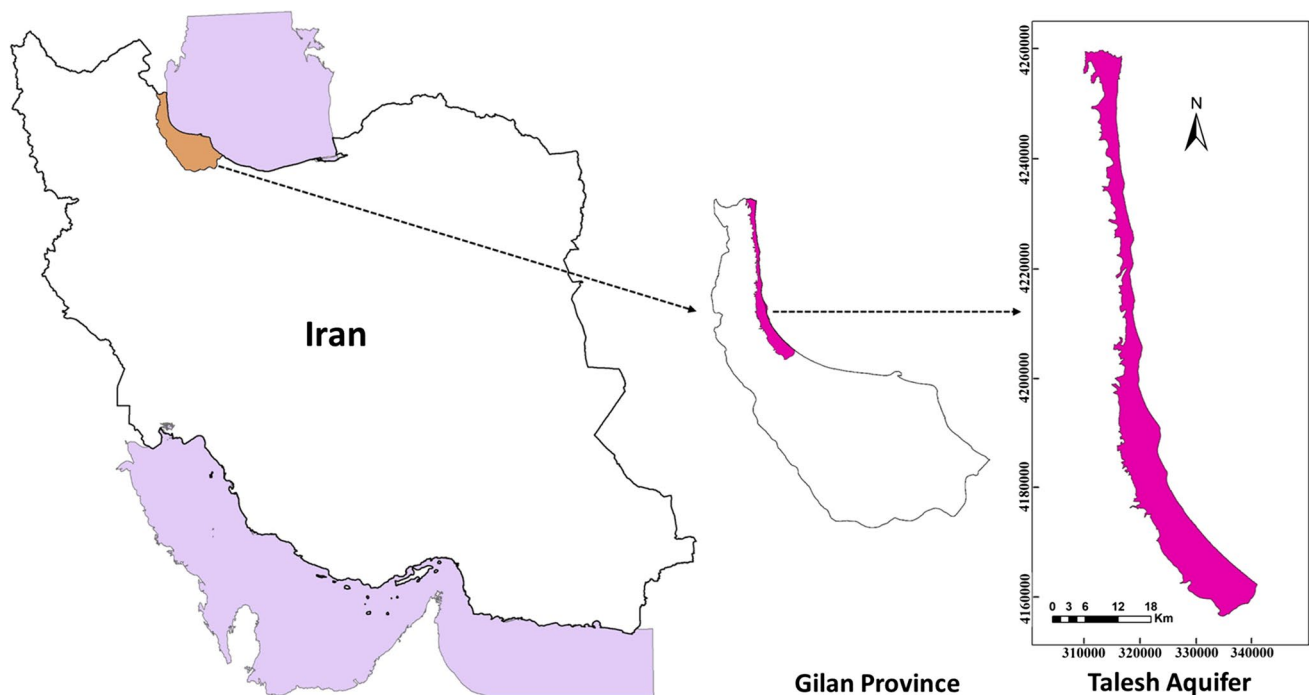


**Fig. 1** Location of the study area in northern Iran

**Table 1** Characteristics of the selected observation wells (piezometers) in the Talesh aquifer

Piezometer	Location		Groundwater level (m)	Pumping rate (m <sup>3</sup> /month)
	X	Y		
P1	314,865	4,255,508	−25.65	−1525.24
P2	311,106	4,253,476	−21.19	−3932.46
P3	311,844	4,246,468	−14.7	−2473.21
P4	313,085	4,240,516	−15.89	−4917.11
P5	315,107	4,232,886	−23.9	−6200.31
P6	316,223	4,226,552	−22.67	−6467.11
P7	316,255	4,219,090	−18.73	−8295.29
P8	315,618	4,209,493	−9.68	−16,988.1
P9	316,101	4,200,099	−5.22	−31,948.9
P10	319,131	4,185,880	−9.84	−51,607.4
P11	324,020	4,175,634	−15.133	−45,348
P12	339,138	4,160,255	−21.99	−38,390.7

RCP2.6 being the lowest (IPCC 2013). The IPCC data distribution center provided temperature and precipitation data for each of the GCMs (<http://www.ipcc-data.org>).

A statistical downscaling method can be used to convert the results of GCMs into usable local meteorological data because they have a large scale (Wilby et al. 2004). For instance, LARS-WG is one of these models, which uses statistical methods for exponential downscaling of meteorological data (Karimi

and Nabizadeh 2018). This model can downscale precipitation (mm), minimum and maximum temperature (°C), and solar radiation (MJ/m<sup>2</sup>/day) for current and future conditions (Semenov 2007; Mohammadloo and Tahmasebipour 2018; Cambraia Neto et al. 2021; El Asri et al. 2019).

For the first step of downscaling, all changes in future monthly data were calculated using Eq. 1

$$F_{\text{fut}} = F_{\text{obs}} + (F_{\text{fut(GCM)}} - F_{\text{base(GCM)}}) \quad (1)$$

where,  $F_{\text{fut}}$  is the future variable change and  $F_{\text{obs}}$  is the average observed variable in the baseline period (1992–2020). Then, LARS-WG by maintaining the average of data changes the standard deviation (STD) according to Eq. 2:

$$F_{\text{fut}} = \frac{STD_{\text{obs}}}{STD_{\text{base(GCM)}}} * STD_{\text{fut(GCM)}} \quad (2)$$

## 2.4 Evapotranspiration

Another variable used in the SVR approach to model the baseline and future period is the potential evapotranspiration ( $P_{\text{ET}}$ ). Since the differences between various methods for estimating potential evapotranspiration have been reported in different regions, including Iran, these methods were prioritized in the following order: (1) Penman–Monteith (PM), (2) Hargreaves–Samani (HS), and (3) Thornthwaite (Beguiria et al. 2014; Shiru et al. 2019). We used the HS method (Eq. 3) to estimate PET in this study as it was more

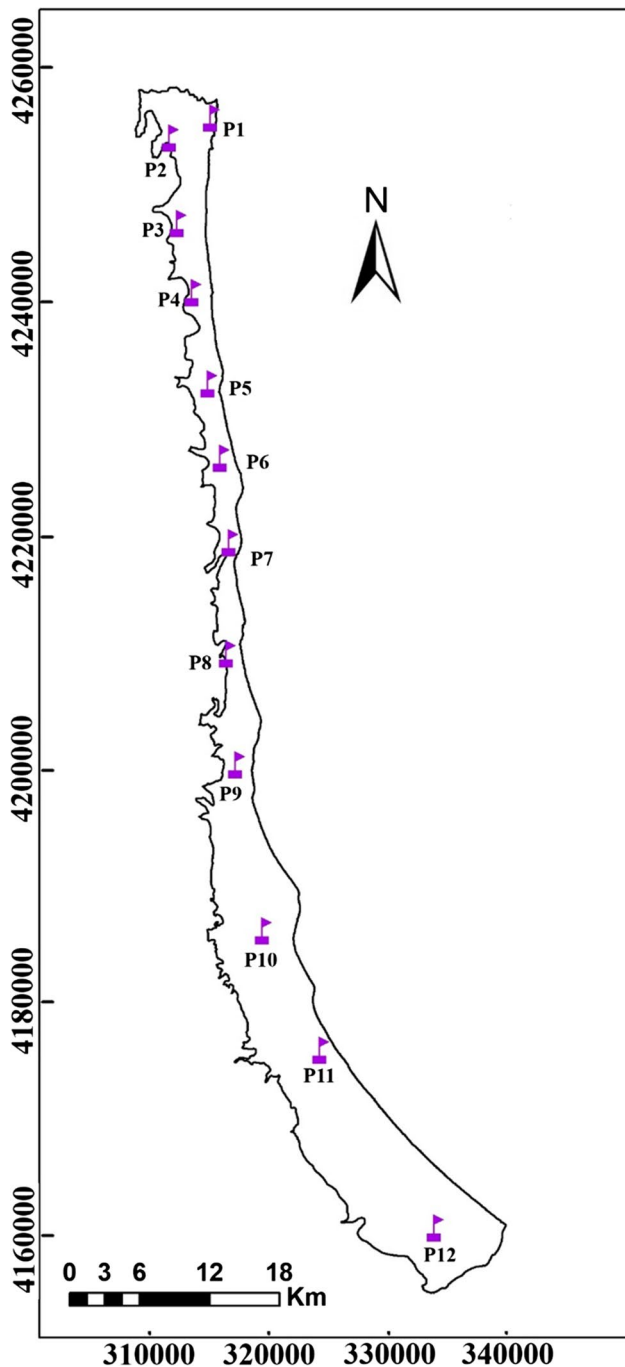


**Fig. 2** Dispersion of selected observation wells (piezometers) in Talesh aquifer

suitable than the PM method in many regions in Iran (Raziei and Pereira, 2013; Hasanzadeh Saray et al. 2020).

$$P_{ET} = 0.0023 \times R_a \times (T_{\max} - T_{\min})^{0.5} \times \left( \frac{T_{\max} + T_{\min}}{2} + 17.8 \right) \quad (3)$$

where  $T_{\max}$  and  $T_{\min}$  are the maximum and minimum air temperature, respectively;  $R_a$  is the solar radiation ( $\text{MJ}/\text{m}^2$ ) obtained according to the latitude of the study area and the Julian day number (Hargreaves and Samani 1985).

## 2.5 GMS model

The MODFLOW is a fully distributed, physics-based, and three-dimensional groundwater model that is widely used worldwide in groundwater resources modeling (Liu et al. 2020; El Yaouti et al. 2008). The calibration of this model is based on groundwater and non-groundwater training data (Chen et al. 2019). There are two types of stress on the groundwater regime: inlet and outlet, where recharge due to precipitation, and return flow from agriculture are the inputs to the aquifer system. On the other hand, the lateral groundwater flow to the inlet, pumping, evapotranspiration, and lateral groundwater flow to the outlet constitutes the outlet of an aquifer system. Groundwater models begin with determining the boundaries of groundwater inflow and outflow (Reilly 2001). The geophysical research conducted in the study area has provided a necessary overview of the aquifer geometry to develop a groundwater model. Generally, creating the conceptual model is the first step in groundwater modeling. Then, the actual physical boundaries of the aquifer must be specified (If such boundaries do not exist, the hydraulic boundaries must be considered). Following that, a grid model is created to divide the aquifer into several cells. In the next step, input parameters and variables (such as altitude, groundwater level, hydraulic conductivity (horizontal and vertical), specific storage, porosity, recharge, evapotranspiration, pumping rate, and river flow) should be defined for the model. It is also necessary to specify other important conditions, such as the lack of boundaries and constant head boundaries. Once the initial conditions are defined, the model is implemented and calibrated by trial and error. The calibration process ends when the root mean square error (RMSE) approaches an acceptable value (Devarajan and Sindhu 2015).

Accordingly, information on 12 observation wells (piezometers), 11,220 pumping wells, hydrodynamic properties of the aquifer, flow boundaries, bedrock of the aquifer, and topography of the area were used to develop the conceptual model of the Talesh aquifer. The model is calibrated using the parameter estimation technique (PEST) and the internal module of MODFLOW (Patil et al. 2020; Kaur et al. 2021). In other words, the MODFLOW model uses the numerical solution of the groundwater flow equation for mathematical simulations of porous medium based on Eq. 4:

$$P \frac{\partial}{\partial X} \left( K_{xx} \frac{\partial H}{\partial X} \right) + \frac{\partial}{\partial y} \left( K_{yy} \frac{\partial H}{\partial y} \right) + \frac{\partial}{\partial z} \left( K_{zz} \frac{\partial H}{\partial z} \right) - W = S_s \frac{\partial H}{\partial t} \quad (4)$$

where  $K_{xx}$ ,  $K_{yy}$ , and  $K_{zz}$  are the hydraulic conductivity along the  $x$ ,  $y$ , and  $z$  axes, respectively;  $H$ : hydraulic head,  $W$ :



volumetric flux per unit volume representing source/sink,  $S_s$ : specific storage of porous material, and  $t$ : time.

## 2.6 Support vector regression

Modeling and predicting data using support vector machines (SVR) is based on classification and regression principles. This type of model is referred to as backup vector regression when it is based on regression. Figure 3 illustrates how an SVR model matches a continuous value function to the observed data. In the regression problem model, the inputs (pumping values, piezometric well level, precipitation, and evapotranspiration) are plotted into a multidimensional space, and the SVR is trained according to the structural risk minimization (SRM) principle. Inputs are mapped to a higher dimension space by a kernel function. When the data set of  $((x_1, t_1), \dots, (x_n, t_n))$  is considered as training data (where  $x$  is the model input and  $t$  is the target),  $x$  SVR algorithm attempts to estimate a function  $(f(x))$  that deviates less than  $\varepsilon$  from the observed target  $y_i$  for all input data values ( $\varepsilon$  is a precision parameter representing the radius of the tube located around the regression function  $(f(x))$ ). The SVR is a popular MLA developed based on the concept of Vapnik (1995). It can be used to model and control complex engineering systems in terms of structure minimization norms (SRMs) that identify each relationship between input and output variables (Eq. 5):

$$Py = W\varphi(x) + b \quad (5)$$

where  $\omega$  and  $b$  represent the weight coefficient and constant coefficient, respectively.  $\varphi(x)$  depicts a nonlinear mapping function in the feature space (Cao et al. 2019).

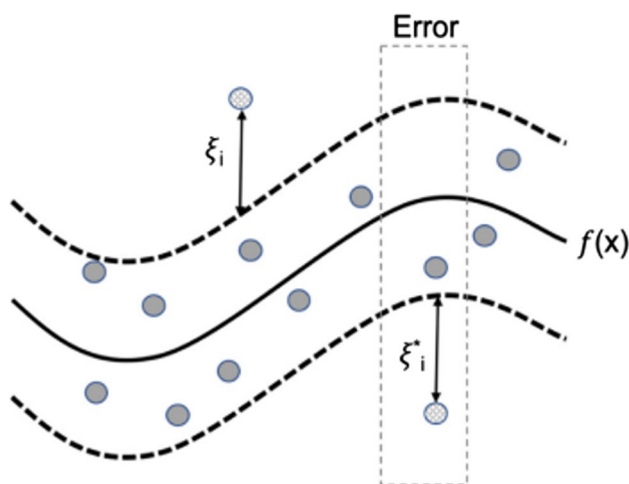


**Fig. 3** Overall framework of Nonlinear Support Vector Regression (SVR) (Osman et al. 2021)

## 2.7 Model performance evaluation

When a training set and an experimental set are used to calibrate the model structure, the performance of the different models can be evaluated by the data match rate. In this study, the coefficient of determination ( $R^2$ ), Nash–Sutcliffe efficiency (NSE), and root mean square error (RMSE) indices were used to evaluate the performance of the models (Eqs. 6–8):

$$RMSE = \sqrt{\frac{\sum_{i=1}^n (O_i - E_i)^2}{n}} \text{ range}[0, \infty] \quad (6)$$

$$NSE = 1 - \frac{\sum_{i=1}^n (O_i - E_i)^2}{\sum_{i=1}^n (O_i - \bar{O})^2} \text{ range}[-\infty, 1] \quad (7)$$

$$R^2 = \frac{\left[ \sum_{i=1}^n (O_i - \bar{O}) \cdot (E_i - \bar{E}) \right]^2}{\left[ \sum_{i=1}^n (O_i - \bar{O})^2 \right]^{0.5} \cdot \left[ \sum_{i=1}^n (E_i - \bar{E})^2 \right]^{0.5}} \text{ range}[0, 1] \quad (8)$$

where  $O_i$  is the observed groundwater level,  $E_i$  is the groundwater level simulated in the base period,  $\bar{O}$  is the average observed groundwater level and  $\bar{E}$  is the average groundwater level simulated in the base period (Wu et al. 2021). It should be noted that these equations are also used to validate the downscaling of climate change data by the LARS-WG model.

## 3 Results

### 3.1 Climate change prediction

LARS-WG model performance for daily precipitation and temperature forecasts from 1992–2020 is shown in Table 2. During the evaluation process, the HadGEM2-es model was tested for its ability to predict daily precipitation and temperature. According to the results, LARS-WG performed well in estimating temperature and precipitation. While the LARS-WG model was able to simulate the temperature pattern better than precipitation based on the calculated RMSE, NSE, and  $R^2$  indices. Figure 4

**Table 2** Results of LARS-WG model evaluation to forecast daily precipitation and temperature during 1992–2020

Weather station	Variable	Evaluation index		
		$R^2$	RMSE	NSE
Talesh	Daily precipitation	0.97	4.15	0.93
	Daily temperature	0.99	0.21	0.99

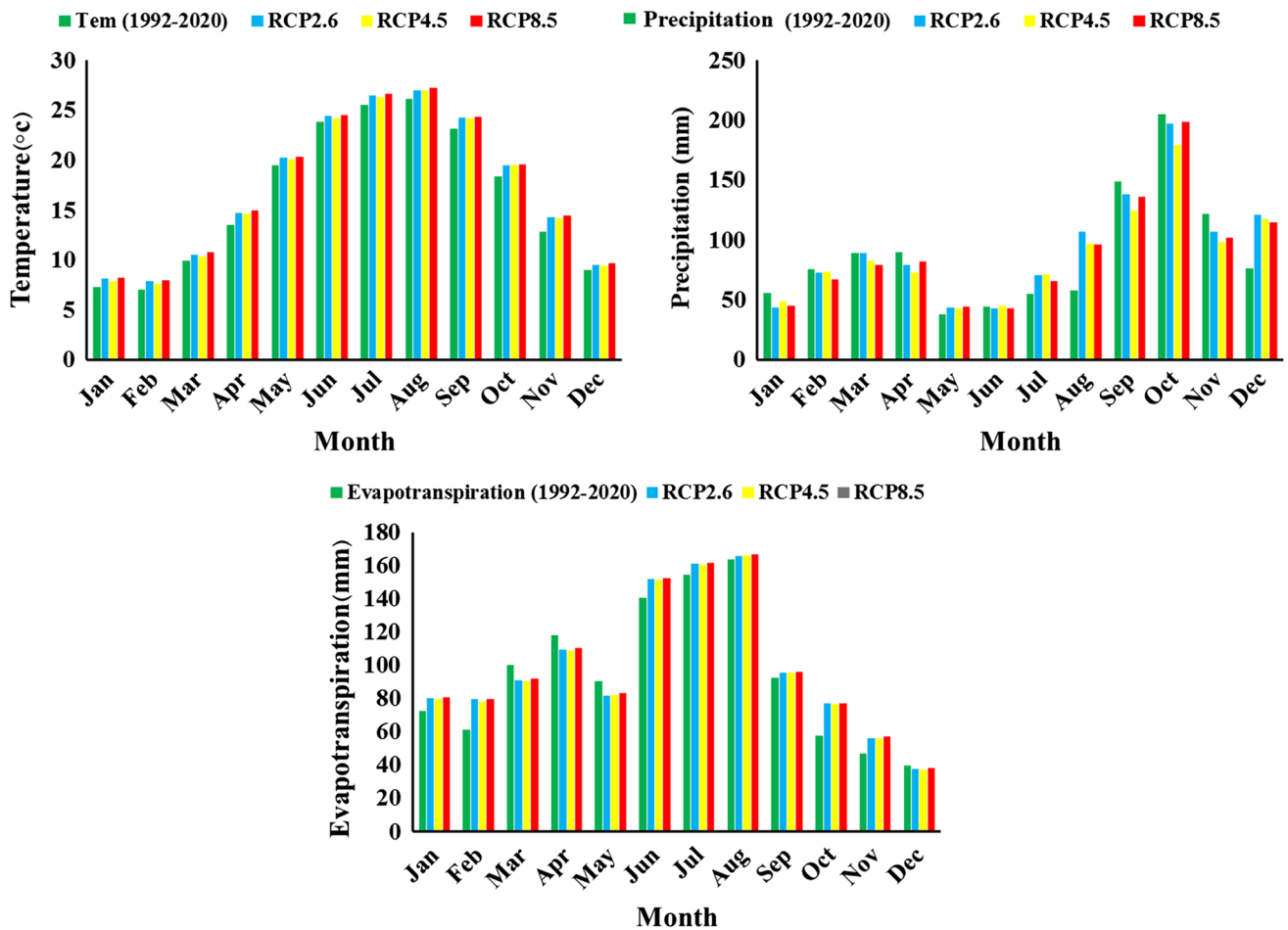


**Fig. 4** Average temperature, precipitation and evapotranspiration changes in the future period (2021–2034) compared to the base period (1992–2020) under different emission scenarios

illustrates the average estimated values of evapotranspiration, precipitation, and temperature in the future under different emission scenarios of RCP2.6, RCP4.5, and

RCP8.5. Furthermore, the changes in these variables in the future compared to the base period can be found in Table 3.

**Table 3** Average temperature, precipitation and evapotranspiration, changes in the future period (2020–2034) compared to the base period (1992–2020) at Talesh weather station for different emission scenarios

Month	Precipitation (%)			Temperature (°C)			Evapotranspiration (%)		
	RCP2.6	RCP4.5	RCP8.5	RCP2.6	RCP4.5	RCP8.5	RCP2.6	RCP4.5	RCP8.5
Jan	12	21	4	1.50	1.10	1.57	11	9	11
Feb	6	10	−7	1.59	1.04	1.70	30	28	30
Mar	18	3	0	1.44	1.08	1.86	−9	−10	−8
Apr	19	1	11	1.35	1.19	1.81	−7	−8	−7
May	5	3	9	1.44	1.22	1.65	−9	−9	−8
Jun	−6	5	−6	1.54	1.20	1.71	8	7	8
Jul	−5	−4	−19	1.59	1.38	1.97	4	4	5
Aug	−1	−18	−19	1.74	1.67	2.17	1	2	2
Sep	−5	−24	−7	1.95	1.91	2.16	3	3	4
Oct	3	−14	4	1.76	1.73	1.98	34	34	35
Nov	29	11	18	1.38	1.27	1.69	20	19	21
Dec	33	27	21	1.31	1.11	1.54	−6	−7	−4

According to the results, August will be the month with the highest temperatures and evapotranspiration. Additionally, the maximum precipitation in all emission scenarios is predicted for October (Fig. 4). Table 3 also shows the changes in these variables compared to the base period. In all emission scenarios, the temperature will increase in all months of the year in the next period. The maximum and minimum temperature increases in the study area were predicted to be 2.17 °C in August for the RCP8.5 emission scenario and 1.04 °C in February for the RCP4.5 emission scenario, respectively. As for changes in precipitation in the future period, it has been shown that precipitation may increase or decrease in different emission scenarios and months of the year. However, this increase will never exceed 33% (in December and RCP2.6). This region is also expected to experience a maximum precipitation reduction of 34% in September under RCP4.5 emissions. Finally, the results indicate that evapotranspiration will fluctuate throughout the year. Evapotranspiration is expected to increase by 35% in October under RCP8.5. However, there will be a maximum reduction of evapotranspiration of 10% in March and RCP4.5 scenarios (Table 3).

Overall, the RCP8.5 emission scenario shows a relatively greater increase in temperature and evapotranspiration than other scenarios. This scenario will also result in a significant decrease in precipitation. Nevertheless, the maximum decrease in precipitation is predicted to occur during the warmest months of the year, so total annual precipitation is not expected to change significantly in future periods.

**Table 4** Evaluation of the GMS and SVR models for groundwater level simulation

Model	Evaluation index		
	NSE	$R^2$	RMSE
GMS	0.86	0.89	2.41
SVR	0.70	0.72	3.37

**Table 5** Evaluation of the GMS and SVR model evaluations for groundwater level simulation in different piezometers

Piezometer	GMS			SVR		
	$R^2$	RMSE	NSE	$R^2$	RMSE	NSE
P1	0.82	0.20	0.83	0.75	0.15	0.72
P2	0.92	0.21	0.86	0.85	0.39	0.80
P3	0.77	0.10	0.75	0.65	0.17	0.64
P4	0.96	0.23	0.88	0.67	0.46	0.65
P5	0.87	0.25	0.79	0.85	0.27	0.80
P6	0.93	0.16	0.90	0.71	0.27	0.70
P7	0.76	0.51	0.72	0.78	0.50	0.74
P8	0.85	0.73	0.80	0.80	0.45	0.78
P9	0.85	0.35	0.79	0.96	0.19	0.88
P10	0.69	0.28	0.63	0.86	0.18	0.83
P11	0.70	0.36	0.66	0.82	0.28	0.80
P12	0.92	0.18	0.90	0.75	0.29	0.71

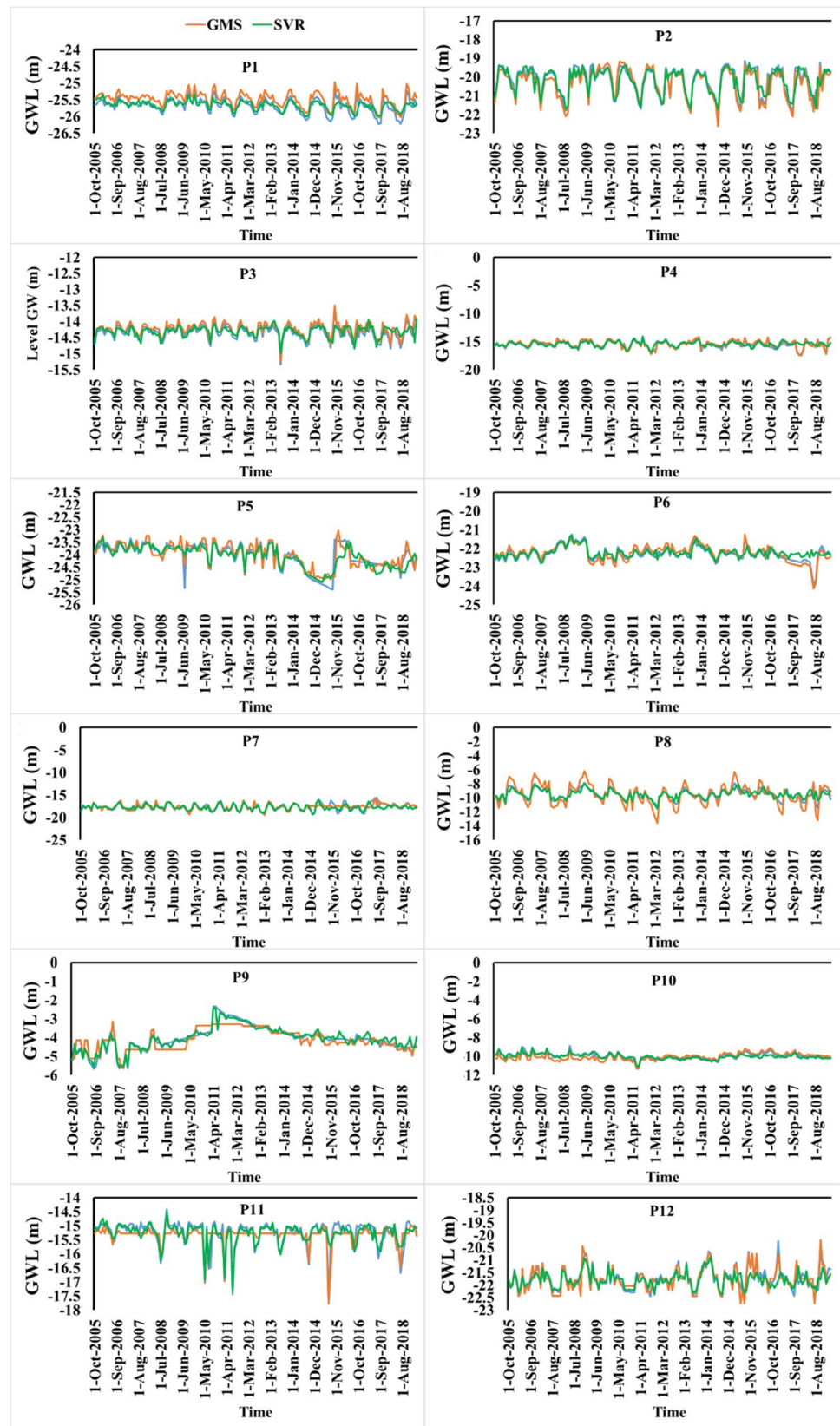
### 3.2 Groundwater modeling

The performance of GMS and SVR models for simulation of groundwater level in the Talesh aquifer was shown in Table 4. According to the results, the calculated NSE,  $R^2$ , and RMSE indices for the GMS method are 0.86, 0.89, and 2.41, respectively. The same parameters for SVR calibration were obtained as 0.70, 0.72, and 3.37, respectively. The results reveal that both models have an acceptable ability to simulate groundwater behavior, although the GMS model performs this simulation more accurately (Table 4). Thus, these two models can be used to simulate future fluctuations in groundwater levels as a result of climate change. Furthermore, the calculated  $R_2$  for all piezometers is greater than 0.60 for the SVR and 0.75 for the GMS model evaluations (Table 5), indicating that both models have acceptable validity for predicting groundwater levels in the study area.

Groundwater levels simulated with the GMS and SVR models in various piezometers for the base period are shown in Fig. 5. Furthermore, Fig. 6 depicts the average simulated groundwater levels for the future period using the SVR and GMS models under different emission scenarios. Groundwater levels in the study area dropped on average by 0.86 m during the base period (Fig. 6). In contrast, the groundwater level modeling under RCP2.6, RCP4.5, and RCP8.5 emission scenarios predicted an average groundwater drop of 0.94, 0.98, and 1.04 m, respectively, in the future (2020–2034). Whereas, the same predicted parameters by the GMS model in the future were 0.91, 0.95, and 1.06 m, respectively (Fig. 6). The results showed that groundwater level fluctuations in the study area were more influenced by precipitation changes than by groundwater extraction. The zoning map of groundwater level (GWL) under different conditions and emission scenarios was shown in Fig. 7. According to the results, the northern regions of the study



**Fig. 5** Simulated Groundwater level (GWL) in the base period (2005–2018) using the SVR and GMS models



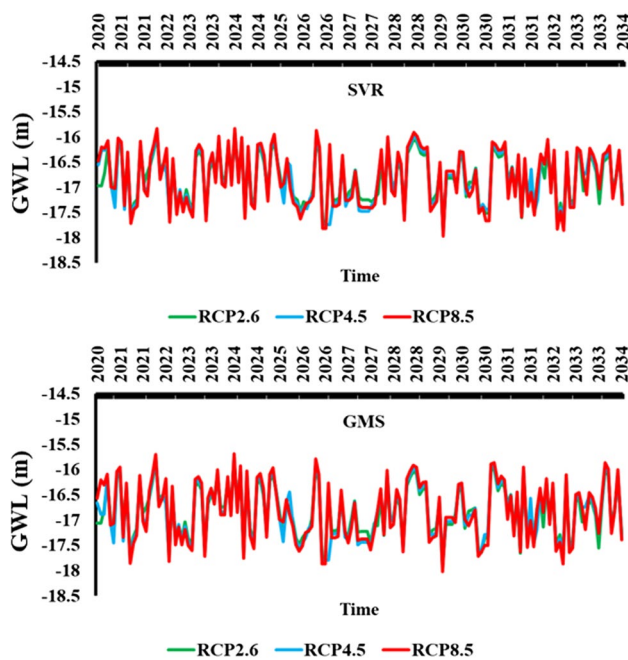


**Fig. 6** Average simulated Groundwater level (GWL) in the future using SVR and GMS models under different emission scenarios

area are more likely to be affected by a decline in groundwater level in the future than other regions (Fig. 7).

To compare the balance simulated by the selected models with the actual groundwater balance of the study area, the latest groundwater balance report of the region (prepared by the Regional Water Company of Guilan Province) in 2018 was used. The regional groundwater deficit is estimated at  $-5.16$  MCMs in the mentioned report. A groundwater deficit of  $-5.30$  MCMs was also calculated using both SVR and GMS methods in 2018 (Table 6). Accordingly, the simulated groundwater balance of Talesh aquifer by these models in the future period and different emission scenarios are presented in Table 7. On average, the groundwater balance in the study area will be negative in the next period, which is estimated by the GMS model in the next period. The values for RCP2.6, RCP4.5, and RCP8.5 emission scenarios were  $-7.36$ ,  $-7.37$ , and  $-7.39$  MCMs, respectively. Whereas for the SVR model, these values were recorded by  $-6.59$ ,  $-6.61$ , and  $-6.63$  MCMs, respectively. Furthermore, for the RCP2.6 scenario, the maximum negative groundwater balance was estimated to be  $-14.62$  MCM in 2032 (Table 7).

## 4 Discussion

According to this study, temperature, precipitation, and evapotranspiration will experience significant fluctuations in the study area in the future period due to climate change, which

is consistent with Crosbie et al. (2009). Therefore, annual precipitation has a significant impact on groundwater recharge. However, in the northern regions of Iran (such as the Talesh Plain), precipitation has the greatest influence on aquifer recharge. McCallum et al. (2010) concluded that the rainy seasons, precipitation intensity, air humidity, air temperature, and actual evapotranspiration are the effective components of groundwater fluctuations. The study results indicate a strong correlation between observed and simulated groundwater levels in both GMS and SVR models (higher than 0.70), which can be attributed to heavy precipitation in the study area leading to rapid recharge of the aquifer (Mukherjee and Ramachandran 2018; Shamsudduha et al. 2012; Panda and Wahr 2016). Based on different statistical indices (RMSE,  $R^2$ , and NSE), there was little difference between the GMS and SVR models in terms of simulated groundwater level fluctuations, but the GMS model performed better because it used aquifer characteristics in its simulation. The inclusion of meteorological variables in groundwater modeling often has significantly improved the quality of the results and the predictive performance of SVR. Nevertheless, this cannot be applied to the GMS model due to the different network structures. To evaluate the potential of SVR for groundwater level prediction, this study divided the available monthly historical groundwater data into two data sets: a training dataset (75% of the total data) and a test dataset (25% of the total data). This resulted in higher accuracy in groundwater level modeling by the two models used. Previous studies have confirmed that using monthly data for groundwater level modeling (including meteorological data such as temperature, precipitation, and evapotranspiration) and groundwater data (such as groundwater levels and pumping rates) can increase the groundwater level modeling efficiency (Sharafati et al. 2020; Choubin and Malekian 2017).

In this study area, the average groundwater decline during the baseline period (2005–2018) was 0.86 m. On the other hand, the simulation of groundwater level in the future (2020–2034) by the SVR model under the RCP2.6, RCP4.5, and RCP8.5 scenarios shows that the groundwater level decreases by 0.94, 0.98, and 1.04 m, respectively. Under the GMS model, this decline is 0.91, 0.95, and 1.06 m, respectively. Our findings are consistent with Gibrilla et al. (2018) who investigated groundwater levels in the Volta River in Ghana and found that the groundwater level drop rate in the study area may increase to 1.1 m per year in the future. Similarly, Patle et al. (2015) predicted future groundwater levels in Haryana, India. They concluded that the groundwater level in the study area will decrease by 12.97 m by 2050 compared to 2010.

Based on the results of this study, machine learning methods (such as SVR) can be used to simulate groundwater levels with acceptable accuracy despite their simplicity. The accuracy of these models, however, is highly dependent on

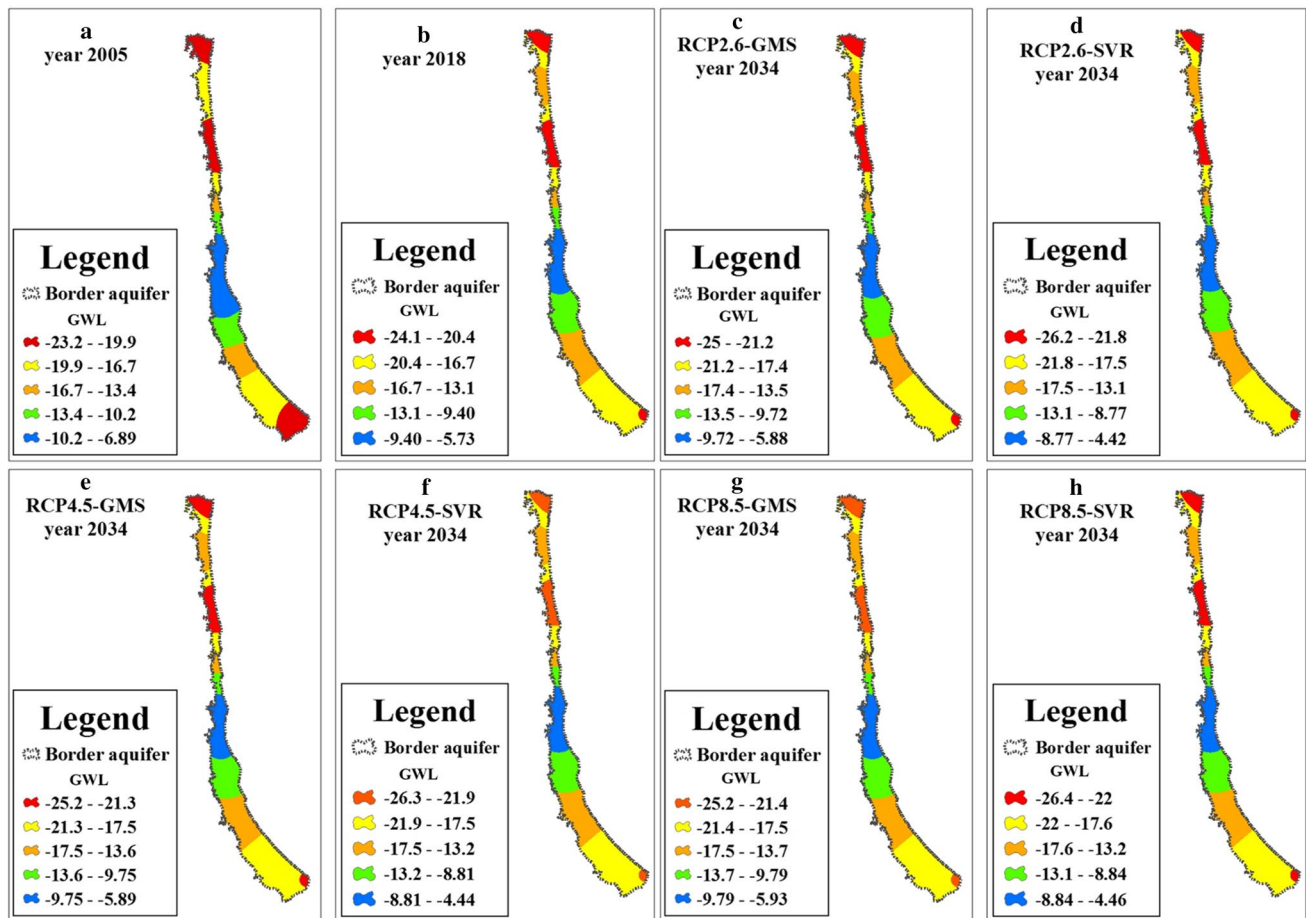


**Fig. 7** Groundwater level zoning map in different conditions and emission scenarios

**Table 6** Estimated groundwater balance in the study area using GMS and SVR models

Outflow (MCM)—SVR	Outflow (MCM)- GMS	Precipitation (mm)	Year
-5.50	-5.28	1115.44	2005
-9.78	-9.51	941.89	2006
5.92	5.59	1387.2	2007
-14.85	-14.69	1001.47	2008
-8.78	-8.59	865.69	2009
0.76	0.98	1122.2	2010
-7.53	-7.46	1032.78	2011
-4.85	-4.72	1055.54	2012
-3.93	-3.76	1118	2013
-5.79	-5.55	1106.73	2014
-5.93	-5.56	1095.15	2015
-10.91	-10.64	875.3	2016
-4.82	-4.15	921.77	2017
1.08	1.75	1209.9	2018
-4.54	-4.06	1259.7	2019
-5.30	-5.04	1073.92	Average

the frequency of the groundwater data used. It is possible to increase the accuracy of these methods if groundwater level data were measured over many years. In this study, only 14 years of groundwater data were available, which is an important limitation. Nevertheless, both methods used to simulate groundwater levels in this study showed acceptable accuracy.

## 5 Conclusions

Throughout the world, groundwater resources are considered strategic water resources that should be carefully used and conserved. Although this issue is not only relevant to arid regions, it is also necessary for humid regions (such as the Talesh Plain). It was found that unmanaged groundwater withdrawals have led to a severe decline in the groundwater level of Talesh Plain, despite significant annual precipitation. According to climate change projections, temperatures and evapotranspiration in the study area will increase in the future, leading to increased water

**Table 7** Estimated Groundwater balance using GMS and SVR models under different emission scenarios

Year	Precipitation (mm)			Total negative balance (Mm <sup>3</sup> )—GMS			Total negative balance (Mm <sup>3</sup> )—SVR		
	RCP2.6	RCP4.5	RCP8.5	RCP2.6	RCP4.5	RCP8.5	RCP2.6	RCP4.5	RCP8.5
2020	1279.4	1193	1237	−7.35	−7.35	−7.35	−6.58	−6.58	−6.58
2021	1272.9	1207.1	1234.3	−7.51	−7.01	−7.42	−6.74	−6.24	−6.65
2022	1039.4	1018.5	985.2	−13.05	−11.95	−13.43	−12.28	−11.18	−12.66
2023	1281.4	1212.1	1242.4	−1.44	−2.63	−1.07	−0.67	−1.86	−0.30
2024	1189	1106	1144.7	−9.60	−9.94	−9.73	−8.83	−9.17	−8.96
2025	1310.2	1258.4	1268.2	−4.39	−3.63	−4.34	−3.62	−2.86	−3.57
2026	1095.7	1052.8	1059.5	−12.58	−12.37	−12.44	−11.81	−11.60	−11.67
2027	827.4	781.1	800.8	−13.90	−13.98	−13.66	−13.13	−13.21	−12.89
2028	743.4	694.5	724.2	−9.40	−9.46	−9.22	−8.63	−8.69	−8.45
2029	1042	987.2	995	−0.06	−0.21	−0.74	0.71	0.56	0.03
2030	1299.9	1221.3	1274.7	−1.06	−1.64	−0.53	−0.29	−0.87	0.24
2031	1040.5	987	1005.9	−13.68	−13.07	−13.91	−12.91	−12.30	−13.14
2032	742.6	704.2	713.6	−14.62	−14.25	−14.48	−13.85	−13.48	−13.71
2033	1209.9	1142.2	1153.7	4.05	3.34	3.39	4.82	4.11	4.16
2034	1259.7	1178.6	1222.4	−6.13	−6.46	−5.67	−5.36	−5.69	−4.90
Average	1108.89	1049.60	1070.77	−7.36	−7.37	−7.39	−6.61	−6.61	−6.63

demand (especially for agriculture). Consequently, water resource managers and policymakers in this area need an efficient and rapid tool to simulate groundwater level changes to facilitate their decision-making. Overall, it can be concluded that the SVR model is capable of simulating groundwater conditions in the study area, although it is simpler and less complex than the GMS model. Hereby, this model can be introduced as a reliable decision-making tool for groundwater management in this region.

**Acknowledgements** This research was supported by the Gilan Regional Water Authority for supplying data for the research.

**Author contribution** This manuscript was taken from the doctoral dissertation of Reza Seraj Ebrahimi. Saeed Eslamian hypothesized and interpreted the results. Reza Seraj Ebrahimi and Mohammad Javad Zareian analyzed the data and wrote the manuscript draft.

**Data availability** The data supporting the results of this study are available upon reasonable request by e-mail to the first author (Reza Seraj Ebrahimi).

**Code availability** Codes will be provided upon reasonable request by e-mail to the first author (Reza Seraj Ebrahimi).

## Declarations

**Ethics approval** It is not involved.

**Consent to participate** Yes.

**Consent for publication** Yes.

**Competing interests** The authors declare no competing interests.

## References

- Affandi AK, Watanabe K (2007) Daily groundwater level fluctuation forecasting using soft computing technique. *Nature and Science* 5(2):1–10
- Alcaraz M, García-Gil A, Vázquez-Suñé E, Velasco V (2016) Advection and dispersion heat transport mechanisms in the quantification of shallow geothermal resources and associated environmental impacts. *Sci Total Environ* 543:536–546. <https://doi.org/10.1016/j.scitotenv.2015.11.022>
- AliNejad A, Gohari A, Eslamian S, Saberi Z (2021) A probabilistic Bayesian framework to deal with the uncertainty in hydro-climate projection of Zayandeh-Rud River basin. *Theoret Appl Climatol* 144:847–860. <https://doi.org/10.1007/s00704-021-03575-3>
- Al-Sheikh A, Hamrah M, Helali M, Fatehi A (2004) Application of GIS in groundwater resources balance of Talesh plain. *Appl Res Geogr Sci (geographical Sciences)* 3(3–4):119–199
- ASCE T (2000) Artificial neural networks in hydrology. I: Preliminary concepts. *J. Hydrol. Eng* 5(2), 115–123. [https://doi.org/10.1061/\(ASCE\)1084-0699\(2000\)5:2\(115\)](https://doi.org/10.1061/(ASCE)1084-0699(2000)5:2(115))
- Barzegar R, Razzagh S, Quilty J, Adamowski J, Pour HK, Booij MJ (2021) Improving GALDIT-based groundwater vulnerability predictive mapping using coupled resampling algorithms and machine learning models. *J Hydrol* 598:126370. <https://doi.org/10.1016/j.jhydrol.2021.126370>
- Beguéría S, Vicente-Serrano SM, Reig F, Latorre B (2014) Standardized precipitation evapotranspiration index (SPEI) revisited: parameter fitting, evapotranspiration models, tools, datasets and drought monitoring. *Int J Climatol* 34(10):3001–3023. <https://doi.org/10.1002/joc.3887>
- Cambraia Neto AJ, Rodrigues LN, da Silva DD, Althoff D (2021) Impact of climate change on groundwater recharge in a Brazilian Savannah watershed. *Theoret Appl Climatol* 143(3):1425–1436. <https://doi.org/10.1007/s00704-020-03477-w>
- Cao L, Xu L, Goodman ED, Bao C, Zhu S (2019) Evolutionary dynamic multiobjective optimization assisted by a support vector



- regression predictor. *IEEE Trans Evol Comput* 24(2):305–319. <https://doi.org/10.1109/TEVC.2019.2925722>
- Chen W, Li H, Hou E, Wang S, Wang G, Panahi M, Ahmad BB (2018) GIS-based groundwater potential analysis using novel ensemble weights-of-evidence with logistic regression and functional tree models. *Sci Total Environ* 634:853–867. <https://doi.org/10.1016/j.scitotenv.2018.04.055>
- Chen W, Tsangaratos P, Ilia I, Duan Z, Chen X (2019) Groundwater spring potential mapping using population-based evolutionary algorithms and data mining methods. *Sci Total Environ* 684:31–49. <https://doi.org/10.1016/j.scitotenv.2019.05.312>
- Chen C, He W, Zhou H, Xue Y, Zhu M (2020) A comparative study among machine learning and numerical models for simulating groundwater dynamics in the Heihe River Basin, north-western China. *Sci Rep* 10(1):1–13. <https://doi.org/10.1038/s41598-020-60698-9>
- Chezgi J, Pourghasemi HR, Naghibi SA, Moradi HR, Kheirkhah Zarkesh M (2016) Assessment of a spatial multi-criteria evaluation to site selection underground dams in the Alborz Province. *Iran Geocarto International* 31(6):628–646. <https://doi.org/10.1080/10106049.2015.1073366>
- Choi JC, Lee SR, Lee DS (2011) Numerical simulation of vertical ground heat exchangers: intermittent operation in unsaturated soil conditions. *Comput Geotech* 38(8):949–958. <https://doi.org/10.1016/j.compgeo.2011.07.004>
- Choubin B, Malekian A (2017) Combined gamma and M-test-based ANN and ARIMA models for groundwater fluctuation forecasting in semi-arid regions. *Environ Earth Sci* 76(15):1–10. <https://doi.org/10.1007/s12665-017-6870-8>
- Crosbie RS, McCallum JL, Harrington GA (2009) Diffuse groundwater recharge modelling across northern Australia, a report to the Australian Government from the CSIRO Northern Australia Sustainable Yields Project. Details Published by CSIRO© 2009 all rights reserved. This work is copyright. Apart from any use as permitted under the Copyright Act 1968, no part may be reproduced by any process without prior written permission from CSIRO. ISSN. <https://doi.org/10.4225/08/585c15f3c4224>
- Cui T, Pagendam D, Gilfedder M (2021) Gaussian process machine learning and Kriging kriging for groundwater salinity interpolation. *Environ Model Software* 144:105170. <https://doi.org/10.1016/j.envsoft.2021.105170>
- Cuthbert MO, Gleeson T, Moosdorf N, Befus KM, Schneider A, Hartmann J, Lechner B (2019) Global patterns and dynamics of climate–groundwater interactions. *Nat Clim Chang* 9(2):137–141. <https://doi.org/10.6084/m9.figshare.7393304>
- Daliakopoulos IN, Coulibaly P, Tsanis IK (2005) Groundwater level forecasting using artificial neural networks. *J Hydrol* 309(1–4):229–240. <https://doi.org/10.1016/j.jhydrol.2004.12.001>
- Das B, Pal SC (2020) Assessment of groundwater vulnerability to over-exploitation using MCDA, AHP, fuzzy logic and novel ensemble models: a case study of Goghat-I and II blocks of West Bengal, India. *Environ Earth Sci* 79(5):1–16. <https://doi.org/10.1007/s12665-020-8843-6>
- Dehghan Z, Eslamian SS, Fathian F, Modarres R (2019) Regional frequency analysis with development of region-of-influence approach for maximum 24-h rainfall (case study: Urmia Lake Basin, Iran). *Theoret Appl Climatol* 136(3–4):1483–1494. <https://doi.org/10.1007/s00704-018-2574-6>
- Dehghan Z, Eslamian SS, Fathian F (2020) Estimation of extreme quantiles at ungaged sites based on region-of-influence and weighting approaches to regional frequency analysis of maximum 24-h rainfall. *Theoret Appl Climatol* 139(44):1191–1205. <https://doi.org/10.1007/s00704-019-03022-4>
- Devarajan K, Sindhu G (2015) Application of numerical and empirical models for groundwater level forecasting. *Int J Res Eng Technol* 4(11):127–133
- Diersch HJ (2005) FEFLOW finite element subsurface flow and transport simulation system. Inst. for Water Resources Planning and System Res, Berlin
- El Asri H, Larabi A, Faouzi M (2019) Climate change projections in the Ghis-Nekkor region of Morocco and potential impact on groundwater recharge. *Theoret Appl Climatol* 138(1):713–727. <https://doi.org/10.1007/s00704-019-02834-8>
- Emamgholizadeh S, Moslemi K, Karami G (2014) Prediction the groundwater level of bastam Plain (Iran) by artificial neural network (ANN) and adaptive neuro-fuzzy inference system (ANFIS) Water resources management 28(15), 5433–5446. <https://doi.org/10.1007/s11269-014-0810-0>
- Eslamian S, Safavi HR, Gohari A, Sajjadi M, Raghbi V, Zareian MJ (2017) Climate change impacts on some hydrological variables in the Zayandeh-Rud River basin. In *Reviving the dying giant*, Springer, Cham, Iran
- Fallah-Mehdipour E, Haddad OB, Mariño MA (2013) Prediction and simulation of monthly groundwater levels by genetic programming. *J Hydro-Environ Res* 7(4):253–260. <https://doi.org/10.1016/j.jher.2013.03.005>
- Fallah-Mehdipour E, Haddad OB, Marino MA (2014) Genetic programming in groundwater modeling. *J Hydrol Eng* 19(12):04014031. [https://doi.org/10.1061/\(ASCE\)HE.1943-5584.0000987](https://doi.org/10.1061/(ASCE)HE.1943-5584.0000987)
- Feng W, Lu H, Yao T, Yu Q (2020) Drought characteristics and its elevation dependence in the Qinghai-Tibet plateau during the last half-century. *Sci Rep* 10(1):1–11. <https://doi.org/10.1038/s41598-020-71295-1>
- Filipe AF, Lawrence JE, Bonada N (2013) Vulnerability of stream biota to climate change in mediterranean climate regions: a synthesis of ecological responses and conservation challenges. *Hydrobiologia* 719(1):331–351. <https://doi.org/10.1007/s10750-012-1244-4>
- Gibrilla A, Anornu G, Adomako D (2018) Trend analysis and ARIMA modelling of recent groundwater levels in the White Volta River basin of Ghana. *Groundw Sustain Dev* 6:150–163. <https://doi.org/10.1016/j.gsd.2017.12.006>
- Gohari A, Zareian MJ, Eslamian S, Nazari R (2017) Interbasin transfers of water: Zayandeh-Rud River basin. CRC Press, In *Handbook of Drought and Water Scarcity*
- Granata F, Gargano R, De Marinis G (2016) Support vector regression for rainfall-runoff modeling in urban drainage: a comparison with the EPA's EPA's storm water management model. *Water* 8(3):69. <https://doi.org/10.3390/w8030069>
- Harbaugh AW, Banta ER, Hill MC, McDonald MG (2000) Modflow-2000, the U. S. geological survey modular ground-water model-user guide to modularization concepts and the ground-water flow process. Open-file report. U. S. Geological Survey (92), 134.
- Hargreaves GH, Samani ZA, (1985) Reference crop evapotranspiration from temperature. *Appl Eng Agric* 1:96–99. <https://doi.org/10.13031/2013.26773>
- Hasanzadeh Saray M, Eslamian SS, Klöve B, Gohari A (2020) Regionalization of potential evapotranspiration using a modified region of influence. *Theoret Appl Climatol* 140:115–127. <https://doi.org/10.1007/s00704-019-03078-2>
- IPCC (2013) In: Stocker TF, Qin D, Plattner GK, Tignor M, Allen S., Boschung J, Nauels A, Xia Y, Bex V, Midgley PM (Eds.), *Climate change 2013: the physical science basis. Contribution of working group I to the fifth assessment report of the intergovernmental panel on climate change*. Cambridge University Press, Cambridge. <https://doi.org/10.1017/CBO9781107415324>



- Jalalkamali A, Sedghi H, Manshouri M (2011) Monthly groundwater level prediction using ANN and neuro-fuzzy models: a case study on Kerman Plain, Iran. *J Hydroinformatics* 13(4):867–876. <https://doi.org/10.2166/hydro.2010.034>
- Javadi S, Saatsaz M, Shahdany SMH, Neshat A, Milan SG, Akbari S (2021) A new hybrid framework of site selection for groundwater recharge. *Geosci Front* 12(4):101144. <https://doi.org/10.1016/j.gsf.2021.101144>
- Karimi M, Nabizadeh A (2018) Evaluation of climate change impacts on climate parameters of Lake Urmia watershed during 2040–2011 using LARS-WG Model. *J Geogr Plann* 22(65):285–267
- Kasiviswanathan KS, Saravanan S, Balamurugan M, Saravanan K (2016) Genetic programming based monthly groundwater level forecast models with uncertainty quantification. *Model Earth Syst Environ* 2(1):27. <https://doi.org/10.1007/s40808-016-0083-0>
- Kaur L, Rishi MS, Singh G, Thakur SN (2020) Groundwater potential assessment of an alluvial aquifer in Yamuna sub-basin (Panipat region) using remote sensing and GIS techniques in conjunction with analytical hierarchy process (AHP) and catastrophe theory (CT) *Ecological Indicators* 110:105850. <https://doi.org/10.1016/j.ecolind.2019.105850>
- Kaur N, Kaur S, Kaur P, Aggarwal R (2021) Impact of climate change on groundwater levels in Sirhind Canal Tract of Punjab, India. *Groundw Sustain Dev* 100670. <https://doi.org/10.1016/j.gsd.2021.100670>
- Koutsoyiannis D (2020) Revisiting the global hydrological cycle: is it intensifying? *Hydrol Earth Syst Sci* 24(8):3899–3932. <https://doi.org/10.5194/hess-24-3899-2020>
- Lal A, Datta B (2019) Multi-objective groundwater management strategy under uncertainties for sustainable control of saltwater intrusion: Solution for an island country in the South Pacific. *J Environ Manage* 234:115–130. <https://doi.org/10.1016/j.jenvman.2018.12.054>
- Langevin CD, Dausman AM, Sukop MC (2010) Solute and heat transport model of the Henry and Hilleke laboratory experiment. *Groundwater* 48(5):757–770. <https://doi.org/10.1111/j.1745-6584.2009.00596.x>
- Li J, Lu W, Wang H, Fan Y, Chang Z (2020) Groundwater contamination source identification based on a hybrid particle swarm optimization-extreme learning machine. *J Hydrol* 584:124657. <https://doi.org/10.1016/j.jhydrol.2020.124657>
- Liu D, Liu C, Fu Q, Li T, Imran KM, Cui S, Abrar FM (2017) ELM evaluation model of regional groundwater quality based on the crow search algorithm. *Ecol Ind* 81:302–314. <https://doi.org/10.1016/j.ecolind.2017.06.009>
- Liu W, Bailey RT, Andersen HE, Jeppesen E, Nielsen A, Peng K, Trolle D (2020) Quantifying the effects of climate change on hydrological regime and stream biota in a groundwater-dominated catchment: a modelling approach combining SWAT-MODFLOW with flow-biota empirical models. *Sci Total Environ* 745:140933. <https://doi.org/10.1016/j.scitotenv.2020.140933>
- Lu H, Tian P, He L (2019) Evaluating the global potential of aquifer thermal energy storage and determining the potential worldwide hotspots driven by socio-economic, geo-hydrologic and climatic conditions. *Renew Sustain Energy Rev* 112:788–796. <https://doi.org/10.1016/j.rser.2019.06.013>
- Mahmoodzadeh D, Karamouz M (2019) Seawater intrusion in heterogeneous coastal aquifers under flooding events. *J Hydrol* 568:1118–1130. <https://doi.org/10.1016/j.jhydrol.2018.11.012>
- Mahmoudpour H, Janat Rostami S, Ashrafzadeh A (2021) Qualitative assessment of the coastal aquifer of Talesh plain using the modified DRASTIC vulnerability model. *J Soil Water Sci (agricultural Science and Technology and Natural Resources)* 24(3):118–197
- Maiti S, Tiwari RK (2014) A comparative study of artificial neural networks, Bayesian neural networks and adaptive neuro-fuzzy inference system in groundwater level prediction. *Environ Earth Sci* 71(7):3147–3160. <https://doi.org/10.1007/s12665-013-2702-7>
- Mao X, Shang S, Liu X (2002) Groundwater level predictions using artificial neural networks. *Tsinghua Sci Technol* 7(6):574–579
- Mayilvaganan MK, Naidu KB (2011) ANN and fuzzy logic models for the prediction of groundwater level of a watershed. *Int J Comput Sci Eng* 3(6):2523–2530
- McCallum JL, Crosbie RS, Walker GR, Dawes WR (2010) Impacts of climate change on groundwater in Australia: a sensitivity analysis of recharge. *Hydrogeol J* 18(7):1625–1638
- Minnig M, Moeck C, Radny D, Schirmer M (2018) Impact of urbanization on groundwater recharge rates in Dübendorf, Switzerland. *J Hydrol* 563:1135–1146
- Moazamnia M, Hassanzadeh Y, Nadiri AA, Sadeghfam S (2020) Vulnerability indexing to saltwater intrusion from models at two levels using artificial intelligence multiple model (AIMM). *J Environ Manage* 255:109871
- Moghaddam DD, Rahmati O, Panahi M, Tiefenbacher J, Darabi H, Haghizadeh A, Bui DT (2020) The effect of sample size on different machine learning models for groundwater potential mapping in mountain bedrock aquifers. *CATENA* 187:104421
- Mohammadloo M, Tahmasebipour N (2018) Assessing the impacts of climate change on climate classifications in parts of northwestern Iran. *Rainwater Surface Systems* 5(17):46–35
- Mohanty AK, Rao VG (2019) Hydrogeochemical, seawater intrusion and oxygen isotope studies on a coastal region in the Puri District of Odisha, India. *CATENA* 172:558–571
- Mohapatra JB, Jha P, Jha MK, Biswal S (2021) Efficacy of machine learning techniques in predicting groundwater fluctuations in agro-ecological zones of India. *Sci Total Environ* 785:147319
- Molina-Giraldo N, Blum P, Zhu K, Bayer P, Fang Z (2011) A moving finite line source model to simulate borehole heat exchangers with groundwater advection. *Int J Therm Sci* 50(12):2506–2513
- Mukherjee A, Ramachandran P (2018) Prediction of GWL with the help of GRACE TWS for unevenly spaced time series data in India: analysis of comparative performances of SVR, ANN and LRM. *J Hydrol* 558:647–658
- Nguyen PT, Ha DH, Avand M, Jaafari A, Nguyen HD, Al-Ansari N, Pham BT (2020) Soft computing ensemble models based on logistic regression for groundwater potential mapping. *Appl Sci* 10(7):2469
- Nosrati K, Van Den Eeckhaut M (2012) Assessment of groundwater quality using multivariate statistical techniques in Hashtgerd Plain, Iran. *Environ Earth Sci* 65(1):331–344
- Nourani V, Mogaddam AA, Nadiri AO (2008) An ANN-based model for spatiotemporal groundwater level forecasting. *Hydrol Process: Int J* 22(26):5054–5066
- Osman AIA, Ahmed AN, Chow MF, Huang YF, El-Shafie A (2021) Extreme gradient boosting (Xgboost) model to predict the groundwater levels in Selangor Malaysia. *Ain Shams Eng J* 12(2):1545–1556
- Pachauri RK, Allen MR, Barros VR, Broome J, Cramer W, Christ R, Van Ypersele JP (2014) Contribution of Working Groups I, II and III to the fifth assessment report of the Intergovernmental Panel on Climate Change. synthesis report (p. 151). Ipcc
- Panda DK, Wahr J (2016) Spatiotemporal evolution of water storage changes in India from the updated GRACE-derived gravity records. *Water Resour Res* 52(1):135–149
- Patil NS, Chetan NL, Nataraja M, Suthar S (2020) Climate change scenarios and its effect on groundwater level in the Hiranyakeshi watershed. *Groundw Sustain Dev* 10:100323
- Patle GT, Singh DK, Sarangi A, Rai A, Khanna M, Sahoo RN (2015) Time series analysis of groundwater levels and projection of future trend. *J Geol Soc India* 85(2):232–242

- Pham HV, Tsai FTC (2016) Optimal observation network design for conceptual model discrimination and uncertainty reduction. *Water Resour Res* 52:1245–1264. <https://doi.org/10.1002/2015WR017474>
- Pourghasemi HR, Sadhasivam N, Yousefi S, Tavangar S, Nazarlou HG, Santosh M (2020) Using machine learning algorithms to map the groundwater recharge potential zones. *J Environ Manage* 265:110525
- Rahman AS, Hosono T, Quilty JM, Das J, Basak A (2020) Multiscale groundwater level forecasting: coupling new machine learning approaches with wavelet transforms. *Adv Water Resour* 141:103595. <https://doi.org/10.1016/j.advwatres.2020.103595>
- Rahmati O, Choubin B, Fathabadi A, Coulon F, Soltani E, Shahabi H, Bui DT (2019) Predicting uncertainty of machine learning models for modelling nitrate pollution of groundwater using quantile regression and UNEEC methods. *Sci Total Environ* 688:855–866. <https://doi.org/10.1016/j.scitotenv.2019.06.320>
- Rakhshandehroo GR, Vaghefi M, Aghbolaghi MA (2012) Forecasting groundwater level in Shiraz Plain using artificial neural networks. *Arab J Sci Eng* 37(7):1871–1883. <https://doi.org/10.1007/s13369-012-0291-5>
- Raziei T, Pereira LS (2013) Estimation of ETo with Hargreaves-Samani and FAO-PM temperature methods for a wide range of climates in Iran. *Agric Water Manag* 121:1–18. <https://doi.org/10.1016/j.agwat.2012.12.019>
- Reilly TE (2001) “System and boundary conceptualization in groundwater flow simulation.” Chapter B8, *Techniques of water-resources investigations*, Book 3, U.S. Geological Survey, Denver, CO, 26. <https://doi.org/10.3133/twri03B8>
- Ren L, Hu Z, Hartnett M (2018) Prediction of coastal surface currents using numerical model and soft computing model. *Energy Procedia* 153:16–21. <https://doi.org/10.1016/j.egypro.2018.10.064>
- Sahoo S, Russo TA, Elliott J, Foster I (2017) Machine learning algorithms for modeling groundwater level changes in agricultural regions of the US. *Water Resour Res* 53(5):3878–3895. <https://doi.org/10.1002/2016WR019933>
- Savichev O, Moiseeva J, Guseva N (2021) Changes in the groundwater levels and regimes in the taiga zone of western Siberia as a result of global warming. *Theoret Appl Climatol* 1–11. <https://doi.org/10.1007/s00704-021-03879-4>
- Semenov MA (2007) Development of high-resolution UKCIP02-based climate change scenarios in the UK. *Agric For Meteorol* 144:127–138. <https://doi.org/10.1016/j.agrformet.2007.02.003>
- Shamsudduha M, Taylor RG, Longuevergne L (2012) Monitoring groundwater storage changes in the highly seasonal humid tropics: validation of GRACE measurements in the Bengal Basin. *Water Resour Res* 48(2). <https://doi.org/10.1029/2011WR010993>
- Sharafati A, Asadollah SB, Neshat A (2020) A new artificial intelligence strategy for predicting the groundwater level over the Rafsanjan aquifer in Iran. *J Hydrol* 591:125468. <https://doi.org/10.1016/j.jhydrol.2020.125468>
- Shiru MS, Shahid S, Chung ES, Alias N (2019) Changing characteristics of meteorological droughts in Nigeria during 1901–2010. *Atmos Res* 223:60–73. <https://doi.org/10.1016/j.atmosres.2019.03.010>
- Šimůnek J, Van Genuchten MT, Šejna M (2016) Recent developments and applications of the HYDRUS computer software packages. *Vadose Zone J* 15(7), vzj2016–04. <https://doi.org/10.2136/vzj2016.04.0033>
- Somogyi V, Sebestyén V, Domokos E, Zseni A, Papp Z (2015) Thermal impact assessment with hydrodynamics and transport modeling. *Energy Convers Manage* 104:127–134. <https://doi.org/10.1016/j.enconman.2015.04.045>
- Sreekanth PD, Geethanjali N, Sreedevi PD, Ahmed S, Kumar NR, Jayanthi PK (2009) Forecasting groundwater level using artificial neural networks. *Curr Sci* 933–939
- Su H, Li X, Yang B, en Z (2018) Wavelet support vector machine-based prediction model of dam deformation. *Mech Syst Signal Process* 110:412–427. <https://doi.org/10.1016/j.ymssp.2018.03.022>
- Trichakis IC, Nikolos IK, Karatzas GP (2011) Artificial neural network (ANN) based modeling for karstic groundwater level simulation. *Water Resour Manage* 25(4):1143–1152. <https://doi.org/10.1007/s11269-010-9628-6>
- Usman M, Qamar MU, Becker R, Zaman M, Conrad C, Salim S (2020) Numerical modelling and remote sensing based approaches for investigating groundwater dynamics under changing land-use and climate in the agricultural region of Pakistan. *J Hydrol* 581:124408. <https://doi.org/10.1016/j.jhydrol.2019.124408>
- Voss CI, Souza WR (1987) Variable density flow and solute transport simulation of regional aquifers containing a narrow freshwater-saltwater transition zone. *Water Resour Res* 23:1851–1866. <https://doi.org/10.1029/WR023i010p01851>
- Wakode HB, Baier K, Jha R, Azzam R (2018) Impact of urbanization on groundwater recharge and urban water balance for the city of Hyderabad, India. *Int Soil Water Conserv Res* 6(1):51–62. <https://doi.org/10.1016/j.iswcr.2017.10.003>
- Wilby R, Charles S, Zorita E, Timbal B, Whetton P, Mearns L (2004) Guidelines for use of climate scenarios developed from statistical downscaling methods. IPCC.
- Wu C, Zhang X, Wang W, Lu C, Zhang Y, Qin W, Shu L (2021) Groundwater level modeling framework by combining the wavelet transform with a long short-term memory data-driven model. *Sci Total Environ* 783:146948. <https://doi.org/10.1016/j.scitotenv.2021.146948>
- Yadav B, Ch S, Mathur S, Adamowski J (2017) Assessing the suitability of extreme learning machines (ELM) for groundwater level prediction. *J Water Land Dev* 32:103–112. <https://doi.org/10.1515/jwld-2017-0012>
- El Yaouti F, El Mandour A, Khattach D, Kaufmann O (2008) Modeling groundwater flow and advective contaminant transport in the Bou-Areg unconfined aquifer (NE Morocco) *J Hydro-Environ Res* 2(3), 192–209. <https://doi.org/10.1016/j.jher.2008.08.003>
- Yoon H, Jun SC, Hyun Y, Bae GO, Lee KK (2011) A comparative study of artificial neural networks and support vector machines for predicting groundwater levels in a coastal aquifer. *J Hydrol* 396(1–2):128–138. <https://doi.org/10.1016/j.jhydrol.2010.11.002>
- Yu X, Michael HA (2019) Offshore pumping impacts onshore groundwater resources and land subsidence. *Geophy Res Lett* 46:2553–2562. <https://doi.org/10.1029/2019GL081910>
- Zaghiyan MR, Eslamian S, Gohari A, Ebrahimi MS (2021) Temporal correction of irregular observed intervals of groundwater level series using interpolation techniques. *Theoret Appl Climatol* 145:1027–1037. <https://doi.org/10.1007/s00704-021-03666-1>
- Zheng C, Wang PP (1999) MT3DMS: a modular three-dimensional multispecies transport model for simulation of advection, dispersion, and chemical reactions of contaminants in groundwater systems; documentation and user's user's guide. (<http://hdl.handle.net/11681/4734>).

**Publisher's note** Springer Nature remains neutral with regard to jurisdictional claims in published maps and institutional affiliations.

Springer Nature or its licensor (e.g. a society or other partner) holds exclusive rights to this article under a publishing agreement with the author(s) or other rightsholder(s); author self-archiving of the accepted manuscript version of this article is solely governed by the terms of such publishing agreement and applicable law.